Journal of Applied Geology, vol. 9(2), 2024, pp. 94–108
DOI: http://dx.doi.org/10.22146/jag.95271

Engineering Geological Characteristics of Planned Construction Area of Section 5 Yogyakarta–Bawen Toll Road, Magelang, Indonesia

Mifthahul Abrar, Daniel Tamado, and I Gde Budi Indrawan*

Department of Geological Engineering, Faculty of Engineering, Universitas Gadjah Mada, Yogyakarta, Indonesia

Received: April 1, 2024 | Accepted: February 17, 2025 | Published online: March 27, 2025

ABSTRACT. This paper presents the results of engineering geological mapping conducted in Section 5 of the Yogyakarta-Bawen toll road and tunnel construction area and its surroundings. This research aimed to evaluate the characteristics of the study area's geomorphology, lithology, and geological structures to assess potential geological hazards during and after the toll road and tunnel constructions. This research was conducted by collecting geomorphological and geological data by surface mapping, which was not done in the previous site investigation. The surface mapping results show that the study area is at the geomorphological units of steep and gentle slope volcanic hills. The study area consists dominantly of tuff and tuff breccia units. At the surface, the rocks are extremely weathered. The geological structures controlling the study area are extensional joints with northwest-southeast and northeast-southwest orientation, consistent with the morphological alignment. Although the study area consists dominantly of hilly morphology and extremely weathered rocks, landslides are rarely observed. This may be attributed to the land use and relatively high friction angle of the weathered pyroclastic rocks comprising this area. The soils produced from weathering pyroclastic rocks in the study area may be susceptible to remoulding. Therefore, cut slopes made for road and tunnel constructions must be designed to prevent change in the soil state.

Keywords: Engineering geology · Toll road · Tunnel · Yogyakarta–Bawen.

1 INTRODUCTION

Knowledge of geological conditions is crucial in tunnel construction, as it determines a tunnel's condition, shape, and cost (Norwegian Tunneling Society, 2014). Therefore, geological investigations, including geomorphology, lithology, and geological structure (Dearman, 1991; Gonzalez de Vallejo and Ferrer, 2011), must be conducted in the construction planning stage.

Section 5 of the Yogyakarta - Bawen toll road, where PT Jasamarga Jogja Bawen will build a road tunnel, is in Losari Village, Magelang Regency, Central Java (Figure 1). The Yogyakarta - Bawen tunnel will consist of 2 tunnels, namely Tunnel A (Yogyakarta direction), located on the east side with a length of 490 m, and Tunnel B (Bawen direction), located on the west side with a length of 510 m. Both tunnels were built to serve as traffic lanes for four-wheeled vehicles crossing the Yogyakarta - Bawen Toll Road.

In the planning stage of road and tunnel construction, the planning consultant has conducted various subsurface geological and geotechnical investigations through geophysical surveys, drilling, and in situ tests (PT. Cipta Strada-KSO, 2022). Although the subsurface investigations that have been carried out are pretty comprehensive, mapping of the surface engineering geology has yet to be carried out. To assess carrying capacity and geological hazards, surface engineering geological mapping is required to comprehensively understand

*Corresponding author: I G. B. INDRAWAN, Department of Geological Engineering, Faculty of Engineering, Universitas Gadjah Mada, Jl. Grafika No. 2 Yogyakarta, Indonesia. E-mail: ...

the construction site's geological conditions (i.e., geomorphology, lithology, and geological structure). The engineering geology mapping results presented in this paper are expected to be an input for road and tunnel construction.

2 Methodology

In this study, five stages of research were carried out: the preparation stage, data collection stage, laboratory analysis stage, data processing and interpretation stage, and manuscript writing stage.

In the preparation stage, problem formulation was carried out by discussing with other authors, conducting literature studies, visiting the study site to determine the geological and geomorphological conditions, and establishing hypotheses based on the data collected at this stage.

The next stage is data collection. This stage is divided into two based on the type of data taken: surface and subsurface. Surface data was obtained by conducting geological mapping focusing on rocks' distribution, the rock weathering level, geomorphological conditions, and existing geological structures. The condition of the rock weathering level is determined by referring to the division of weathering levels by Dearman (1991), as seen in Table 1. Meanwhile, subsurface data is obtained by core logging from several boreholes by observing rock conditions (rocks' distribution and the rock weathering level) and the groundwater depth. The location of observation and data collection points can be seen in Figure 2.

After collecting the primary data, laboratory analysis was conducted on the rock samples. Several tests were carried out during this stage, such as petrography, rock index properties test, and rock strength test. Petrography was conducted on 29 rock samples, both from surface and subsurface data. The rock index properties test used rock density, unit weight, and specific gravity values parameters on eight surface rock samples and four subsurface rock samples. The rock strength test was carried out using the point load method, which refers to the standard ASTM D5731-16 (2016) procedure by making the rock sample into a block shape with dimensions of length x height x width of 5 cm x 4 cm x 3 cm on the surface sample, while the core sample can be tested directly because it meets the requirements of $0.3\ W < D < W$ (W = core width and D = core diameter). The result of the point load test is the Point Load Strength Index (Is50) value, which will be converted to Uniaxial Compressive Strength (USC) by multiplying the Point Load Strength Index (Is50) value with the Strength Conversion Factor (K). The sample in the point load test uses the same sample as the rock index properties test.

Data obtained from primary data collection and laboratory tests will be used for data processing and data interpretation. Geological structure data obtained in geological mapping is extensional joint data only found at four observation points. The extensional joint data is analyzed on a rose diagram using GeoRose software by inputting the measured strike orientation value of the extensional joint. The output of this analysis is the direction of the main force that forms the extensional joint. Geomorphological data was obtained through direct field observation and digital elevation model (DEM) image analysis. On the DEM image, slope analysis was carried out using ArcGIS software to make a slope classification based on the slope range referring to the slope class classification by van Zuidam (1983) in Table 2. In addition, the DEM image also analyzed the morphological alignment pattern in the study area by drawing a striking morphological alignment line. Mapping geomorphological characteristics in the field was conducted by observing the morphology and active geomorphological processes, especially landslides. The output of the geomorphological data analysis is the river flow pattern. The results of petrography are used to divide the lithological units on the geological map and cross-section. The petrographic data was then synergized with rock index properties test data, rock strength test data, and rock weathering condition data to determine the rocks' physical, mineralogical, and engineering characteristics. The conclusion was obtained by integrating all the final data and writing the manuscript.

3 Results and Discussion

The results of the surface mapping that has been conducted show that the study area can be divided into two geomorphological units

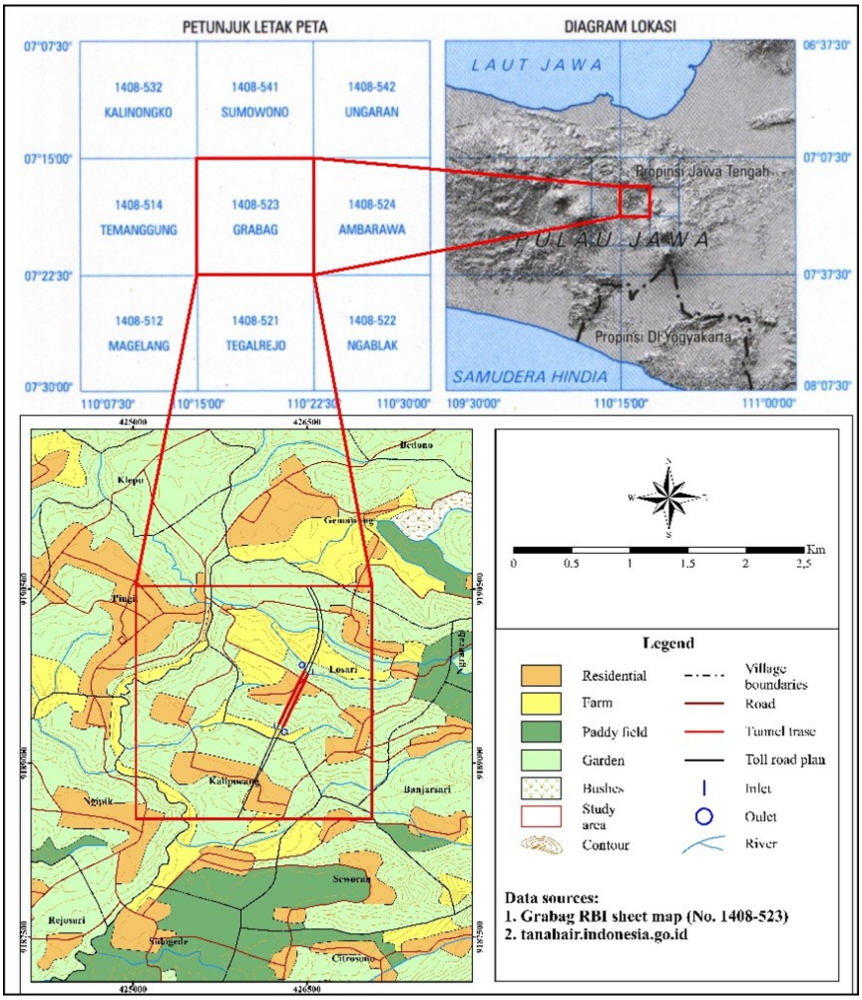

FIGURE 1. The study area is based on the Grabag landform map sheet (No. 1409-523). Map source: https://tanahair.indonesia.go.id/.

TABLE 1. Scale of weathering grades of rock mass (Dearman, 1991).

Term	Description	Grade
Fresh	There is no visible sign of rock material weathering; perhaps slight discoloration on major discontinuity surfaces.	I
Slightly weathered	Discoloration indicates weathering of rock material and discontinuity surfaces. All rock material may be discolored by weathering.	II
Moderately weathered	Less than half of rock material is decomposed or disintegrated into soil. Fresh or discolored rock is present as a continuous framework or as corestones.	III
Highly weathered	More than half of the rock material decomposed or disintegrated into soil. Fresh or discolored rock is present either as a discontinuous framework or as corestones.	IV
Extremely weathered	All rock material decomposed and/or disintegrated to soil. The original mass structure is still largely intact.	V
Residual Soil	All rock material is converted to soil. Mass structure and material fabric destroyed. There is a large change in volume, but soil has not been significantly transported.	VI

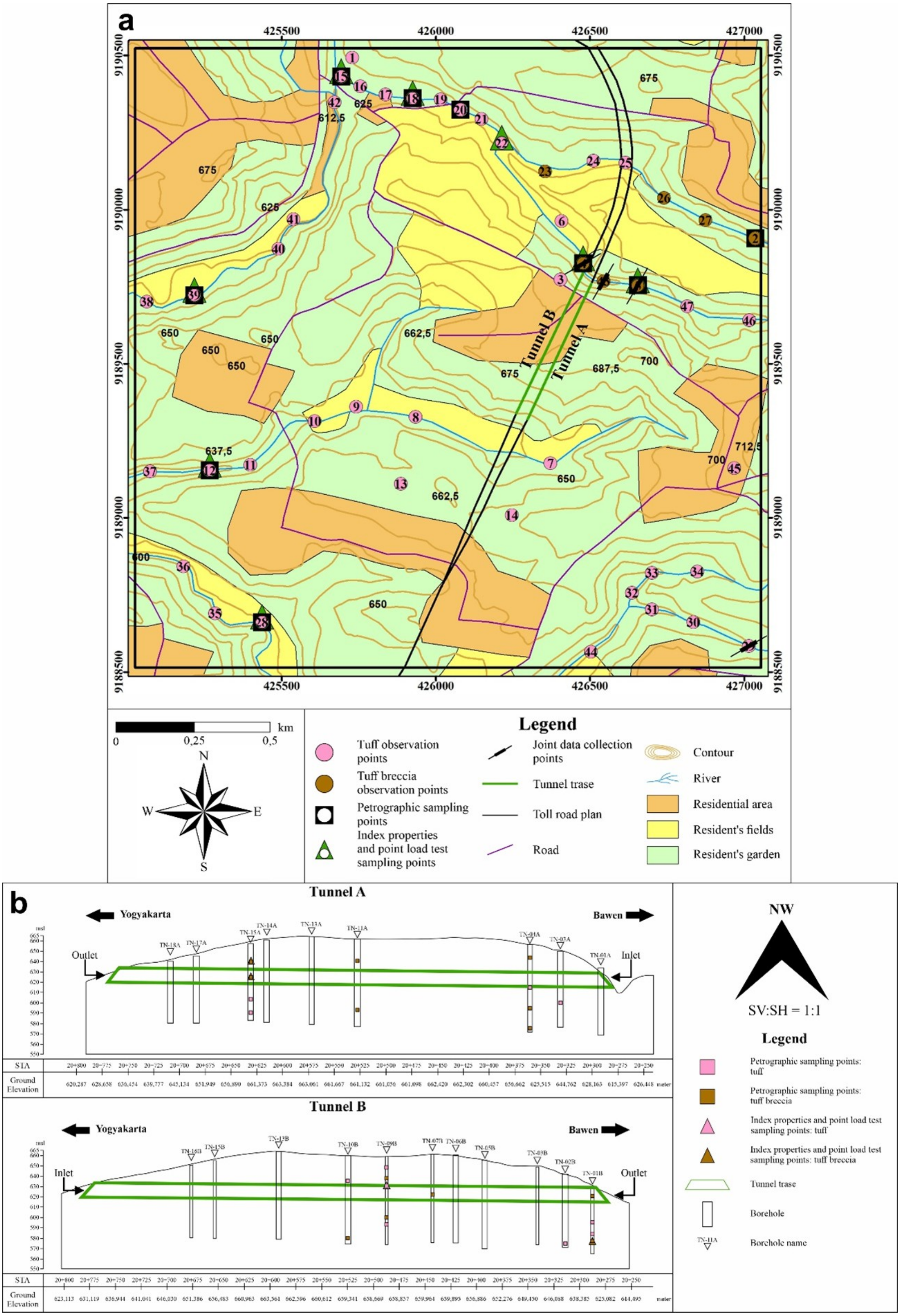

FIGURE 2. The location of observation and data collection points. (a) Surface observation and data collection points. (b) Subsurface data collection points.

Table 2. Slope class classification (van Zuidam, 1983).

Slope class		Process Characteristics and Field Conditions	
Slope angle (. . . °)	Percentage (. . . %)	Classification	Descriptions
0 – 2	0 – 2	Flat to almost flat	There is no meaningful denudation process.
2 – 4	2 – 7	Gentle	Ground motion speed is low. Sheet and soil erosions are identified.
4 – 8	7 – 15	More gentle	The same as above, but with a higher magnitude.
8 – 16	15 – 30	Slightly steep	Flat landslides with a lot of ground movement and erosion.
16 – 35	30 – 70	Steep	Intensive denudation processes and ground movements are common.
35 – 55	70 – 140	Very steep	Rock generally begins to unfold, and a very intensive denudational process has already started to produce rework material.
>55	>140	Extremely steep	Exposed rocks are a very strong denudational process prone to falling rocks; plants are rarely grown (limited).

and two geological units. In addition, in the study area, the geological structure is found as an extensional joint with two orientation directions based on rose diagram analysis. In explaining geomorphological characteristics, several aspects are presented, such as the division of geomorphological units, the division of drainage flow patterns, and the direction of geomorphological alignment. For geological characteristics, results are presented by dividing lithological units based on physical and mineralogical characteristics, dividing the degree of weathering, and engineering characteristics based on the degree of weathering. Meanwhile, the geological structural characteristics explain the structures found and the results of structural analysis using rose diagrams.

3.1 Geomorphological characteristics

The geomorphological condition of an area is a manifestation of geological processes (endogenic and exogenic processes) that work in the area. In the study area, the endogenic process can be reflected through the distribution of lithology and the presence of geological structures, such as extensional joints, that indicate a tectonic activity that works regionally. Meanwhile, the exogenic process in the study area can be reflected through the erosion stadia in the river that developed and the level of weathering recorded in the lithology that makes up the study area and its surroundings.

The study area has the lowest point with an elevation value of 608 meters above sea level, with the highest point reaching 723 meters above sea level. Based on the classification of morphographic elements proposed by van Zuidam (1983), the study area is categorized as hills. This hilly morphology is part of the circular morphology east of the study area (Figure 3). Poedjoprajitno (2011) states that the circular morphology is the crater of an ancient volcano.

Based on the analysis of DEM images (as shown in Figure 3), the study area is located adjacent to two faults, i.e., the Rawapening Fault and the Merapi-Merbabu Fault, and four volcanoes, i.e., Ancient Volcano (Poedjoprajitno, 2011), Mount Merbabu, Mount Andong, and Mount Telomoyo. The Rawapening Fault is a thrust fault, one of the segments of the Baribis-Kendeng Fold-Thrust Zone, while the Merapi-Merbabu Fault is a strike-slip fault (The National Center for Earthquake Studies, 2017). Both are active faults with a movement of 0.1 mm/year (The National Center for Earthquake Studies, 2017). Poedjoprajitno (2011), in the photo geomorphology map of Java and Madura islands, classified the study area into the geo-

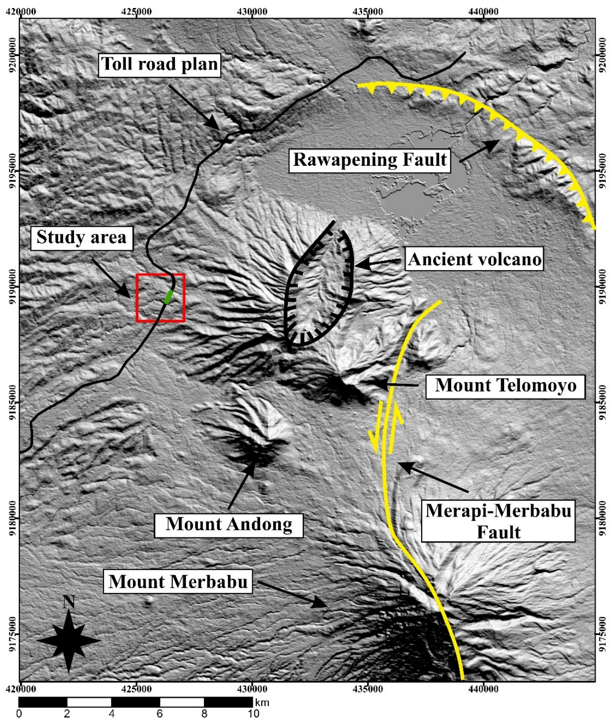

FIGURE 3. DEM image of the study area and its surroundings showing morphological conditions and the location of active faults according to The National Center for Earthquake Studies (2017). DEM source: https://tanahair.indonesia.go.id/.

morphological unit of the ancient volcanic cone where the constituent lithology is sourced from the eruption of the ancient volcano located in the east of the study area.

The slope at the study site is categorized into gentle and steep slopes. This gentle slope is generally found in residential areas, gardens, residents' farms, and cross-village roads made by cutting a hill. Meanwhile, steep slopes are generally found in several places that have yet to be touched by residents due to the difficulty of access to the location. So that the area still shows its original condition without any significant morphological changes by humans. Referring to van Zuidam's (1983) geomorphological unit names and morphometric elements as complementary elements to make the unit names more detailed and can be mapped, the study area can be divided into two geomorphological units, namely the gentle-slope volcanic hills unit (3° – 7°) and the steep-slope volcanic hills unit (7° – 30°) (Figure 4). Several landslides were observed in the steep-slope volcanic hills unit. These landslides are located close to the river, most of which are shallow. Landslides with large dimensions were only found at one point, at the northern part of the outlet of tunnel B. The landslide morphology is shown in Figure 5.

The proximity of the study area to the center of ancient volcanism, the natural slope and lithology types that are relatively uniform, and the morphology of the elongated hills support the formation of parallel drainage patterns (Figure 6a). The orientation of the drainage pattern is consistent with the NE–SW and NW–SE morphological alignment pattern (Figure 6b), suggesting the morphological alignment in the study area to be mainly controlled by erosion rather than tectonics. Tectonic activity on active faults around the study area only resulted in the formation of extensional joints at several observation points. In contrast, erosional activity has an important role in the morphology formation process, such as the development of river stadia in the study area.

3.2 Lithological characteristics

The study area is included in the Geological Map of Magelang and Semarang Sheets, Java, at a scale of 1:100,000 (Thandean *et al.*, 1996). Based on the geological map created by Thandean *et al.* (1996), the study area and its surroundings are composed of Kaligetas Formation (Qpkg), Gilipetung Volcanic Rocks (Qg), and Merbabu Volcanic Rocks (Qme). Kaligetas Formation (Qpkg) is the oldest formation in the study area and its surroundings. This formation comprises lithologies of volcanic breccia, lava flows, tuffaceous sandstone, claystone, flow breccia and lava with lava inserts, and fine to coarse tuff. Gilipetung Volcanic Rocks (Qg) is a formation unit composed of lava flow lithology with a grey and vesicular structure. Merbabu Volcanic Rocks (Qme) is a unit formation comprising olivine basalt and andesite augite lithologies.

The study area is about 6 km from the morphological center of the ancient volcanic crater. The study area is estimated to be in the proximal zone of the volcanic facies based on Bogie and Mackenzie (1998). According to Bogie and Mackenzie (1998), the proximal zone of volcanic facies will be composed of lithologies such as lava, tuff breccia, and lapilli tuff. The results

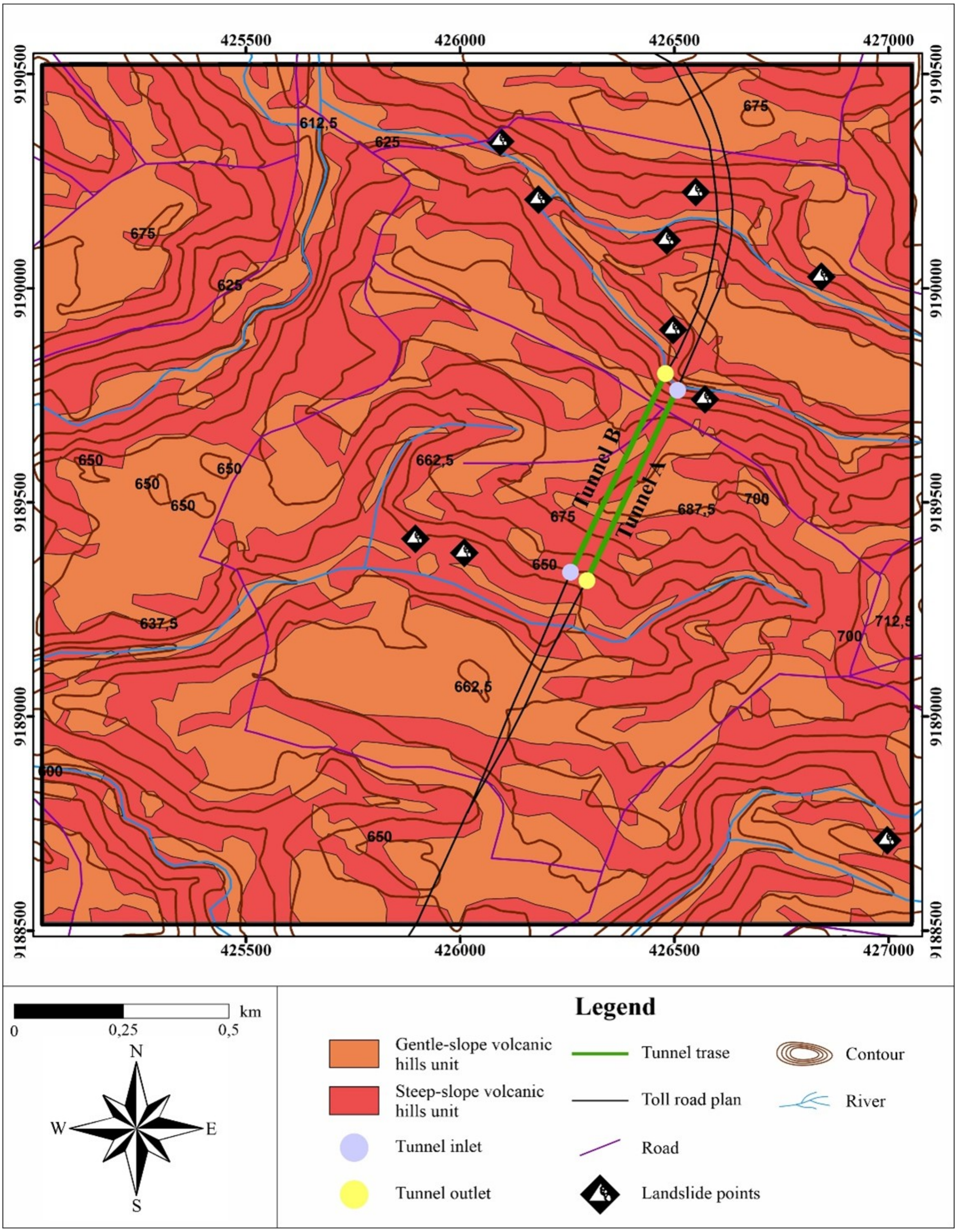

FIGURE 4. Geomorphological map of the study area.

FIGURE 5. Typical landslide observed in the study area.

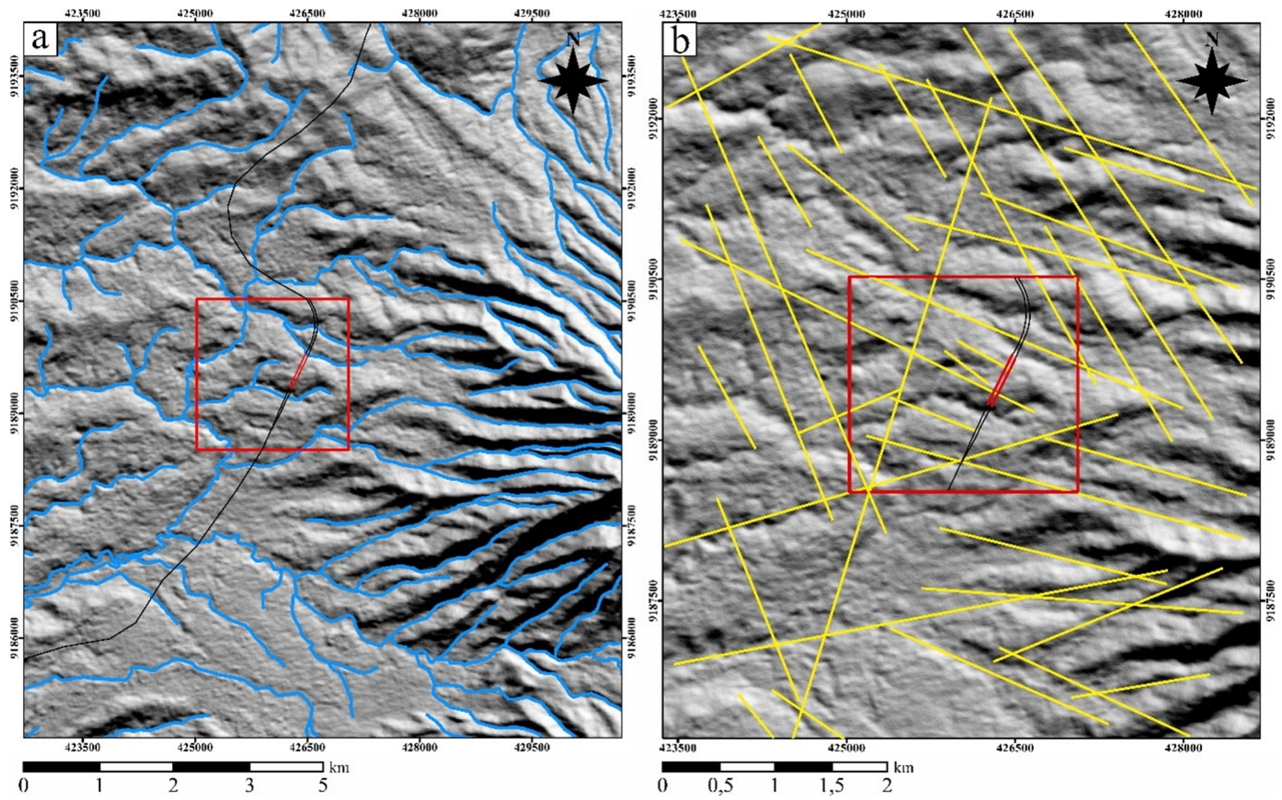

FIGURE 6. DEM image of the study area and its surroundings. (a) Drainage pattern that shows a parallel pattern. (b) Morphological alignment that has an NW-SE and NE-SW direction.

of surface mapping show that the study area is composed of tuff and tuff breccia (Figure 7a). Likewise, the results of core logging conducted on cores from several boreholes along the tunnel route show that the constituent lithologies of the tunnel route are tuff and tuff breccia (Figure 7b).

3.2.1 *Tuff unit*

The tuff unit is produced from a volcano's volcanism process near the study area. This unit has a distribution of about 85% on the surface of the study area. This unit has two types of rocks: crystal tuff and lithic tuff. Lithic tuff in this unit has a very limited distribution and is only found locally.

a. Crystal tuff

Megascopically, this rock has a grain size of <2 mm (very fine) and a sub-rounded to subangular grain shape; the matrix of this rock is composed of hornblende and clay minerals, while the fragments of this rock are composed of lithics from igneous rock fragments and iron oxide minerals. This rock has a massive structure.

Microscopically, this rock has a grain size of <2 mm – 3 mm, has a massive structure, has a sub-rounded to sub-angular grain shape, and the rock composition is lithic, quartz, hornblende, clay minerals, and iron oxide minerals. The rock matrix is composed of hornblende and clay minerals. Fragments are composed of lithics and iron oxide minerals. The naming of lithic tuff is based on Fisher's classification (1966). In the study area, two types of crystal tuff have differences in massive and vesicular structures (Figure 8). At the surface, the crystal tuff is dominantly extremely weathered. Highly weathered tuff is only observed at the river slopes. The engineering properties of the weathered crystal tuff are shown in Table 3. Of particular note are the density values, which are typical for weathering products of pyroclastic rocks. According to the International Society for Rock Mechanics and Rock Engineering (ISRM) (1978), crystal tuff is classified as a very weak rock.

b. Lithic tuff

This rock has a very restricted distribution in the study area. Megascopically, this rock has a grain size of <2 mm and a rounded to subangular grain shape; the matrix of this rock is composed of hornblende and clay minerals, while the fragments of this rock are composed of lithics from igneous rock fragments, mafic minerals, and iron oxide minerals. This rock has a laminated structure.

Microscopically, this rock has a grain size of <2 mm – 3 mm, has a laminated structure, has a sub-rounded to sub-angular grain shape, and the rock composition is lithics, quartz, volcanic glass, hornblende, clay minerals, and iron oxide minerals. The rock matrix comprises volcanic glass, hornblende, and clay minerals. Fragments are composed of lithics and iron oxide minerals. The quartz in this rock is present as veins that fill fractures in the rock. The fractures are so minor that they cannot be seen on a megascopic view. The lithic tuff is named after Fisher's classification (1966). The outcrop, hand specimen sample, and microscopic observations of the lithic tuff can be seen in Figure 9. At the surface, the lithic tuff is mostly highly weathered.

3.2.2 *Tuff breccia unit*

Based on the surface geological mapping results, this unit is below the tuff unit. On the surface, it covers about 15% of the study area.

Megascopically, this rock has a brown color with a massive structure, fragments of andesite with a size of 1–20 cm, and mafic minerals with a size of 5–7 mm; the matrix in this rock is in the form of volcanic material <5 mm in size consisting of clay minerals, sub-angular to subrounded grain shape, and poor sorting. The andesite fragments have a massive structure, porphyro-afanitic granularity texture, and allotriomorphic intercrystal relationship texture, with the constituent composition being plagioclase, mafic minerals, and clay minerals. The percentage of matrix in this breccia is about 65%, and the fragments are about 35%. Based on the rate of fragments and matrix, it can be seen that this rock has the name tuff breccia (Fisher, 1966).

Based on microscopic observations made on the matrix, this rock has a grain size of

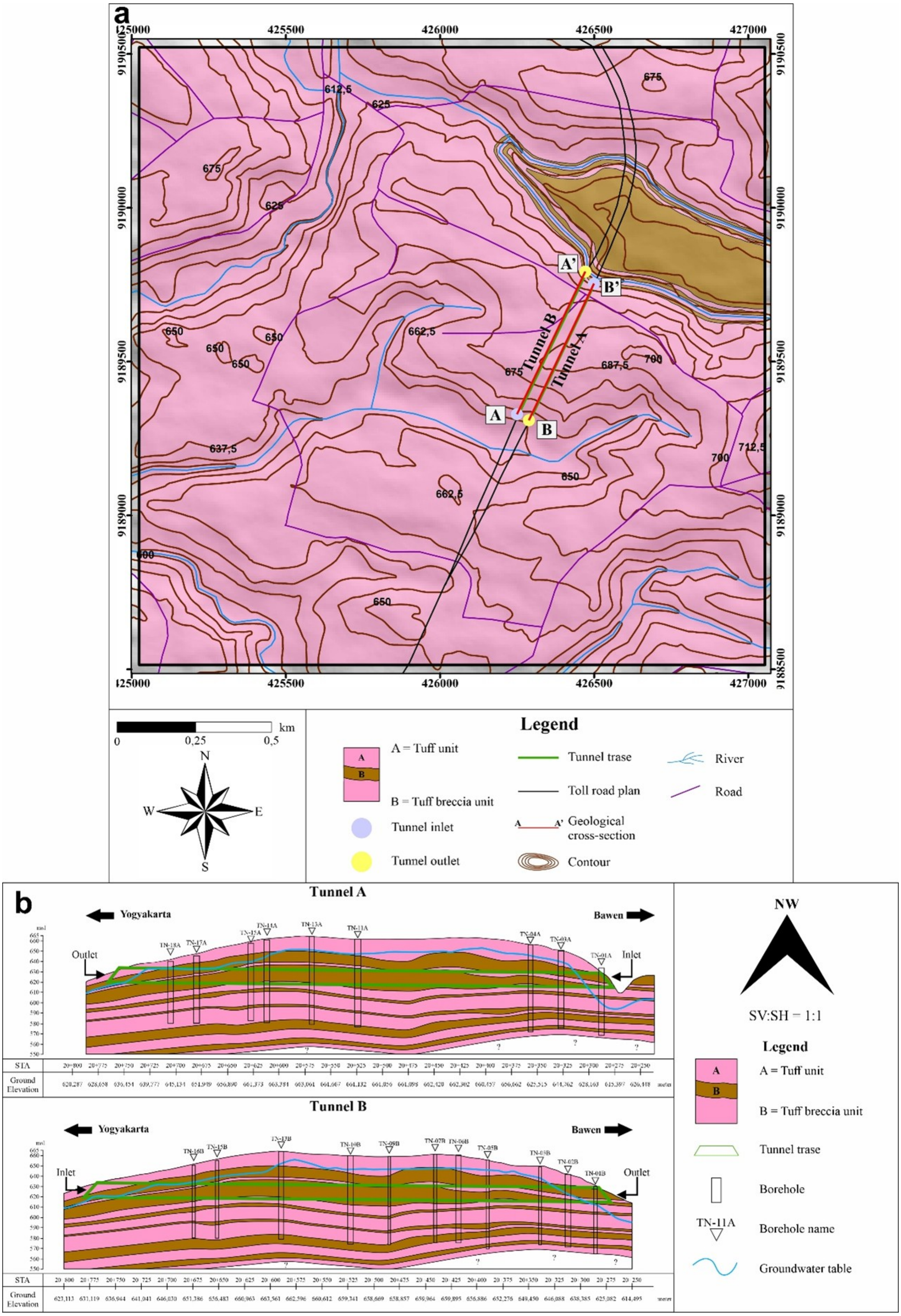

FIGURE 7. (a) Geological map of the study area. (b) Geological cross-section of the tunnel route.

FIGURE 8. (a) Outcrop of massive crystal tuff. (b) Outcrop of vesicular crystal tuff. (c) hand specimen sample of massive crystal tuff. (d) Hand specimen sample of vesicular crystal tuff.

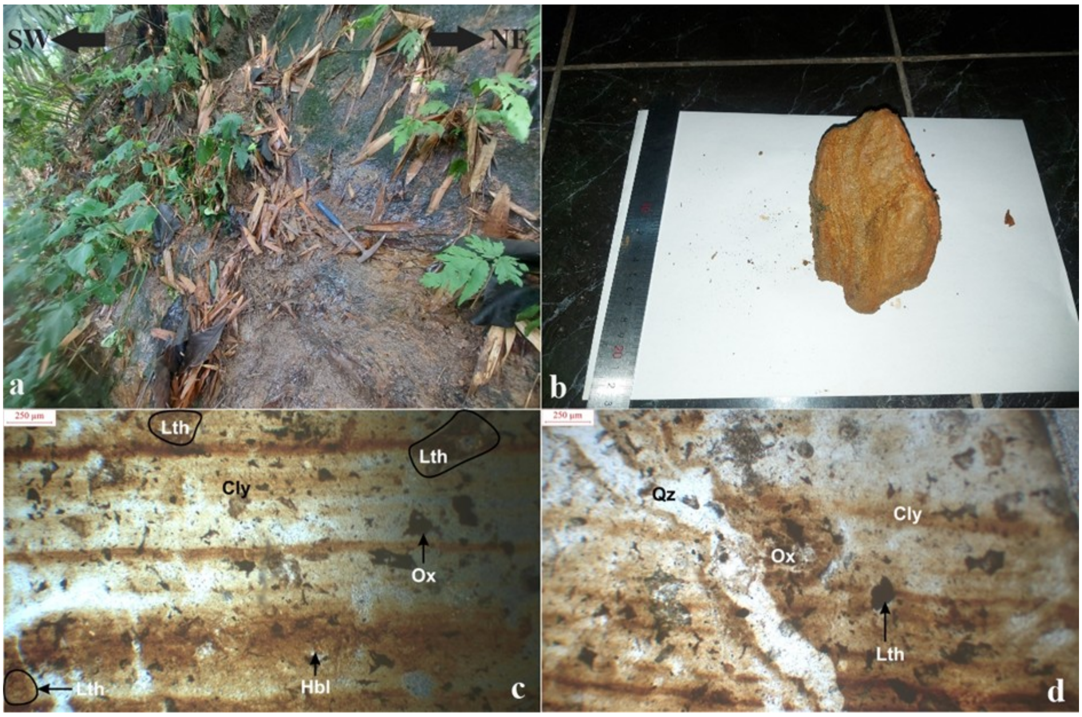

FIGURE 9. (a) Outcrop of lithic tuff. (b) hand specimen sample of lithic tuff. (c) Microphotograph of lithic tuff showing laminated structure. (d) Microphotographs of lithic tuff show a quartz vein filling the micro-fracture. Hbl = hornblende, Cly = clay, Ox = oxide minerals, Lth = lithic, and Qz = quartz.

TABLE 3. Physical, mineralogical, and engineering characteristics of rocks.

Lithological unit	Physical and mineralogical properties	Engineering properties
Highly weathered tuff	Brown in color with massive, vesicular, and laminated structures, fragments are composed of lithics, mafic minerals, and plagioclase with a size of 1 – 3 mm, matrix composed of clay minerals <1 mm in size, sub-angular to sub-rounded grain shape, and medium sorting. The degree of weathering of this rock is highly weathered.	Dry density values range from 1.2 to 1.6 gr/cm3, and compressive strength values range from 1.3 to 1.6 MPa.
Extremely weathered tuff	Brown in color with massive, vesicular, and laminated structures, fragments are composed of lithics, mafic minerals, and plagioclase with a size of 1 – 3 mm, matrix composed of clay minerals <1 mm in size, sub-angular to sub-rounded grain shape, and medium sorting. The degree of weathering of this rock is extremely weathered.	Dry density values range from 1.0 to 1.3 gr/cm3, and compressive strength values range from 1.0 to 1.8 MPa.
Highly weathered tuff breccia	Brown in color with a massive structure, fragments consist of andesite with 1 – 8 cm in size. The matrix comprises clay minerals, plagioclase, and mafic minerals <1 mm in size, sub-angular to sub-rounded grain shape, and poor sorting. Fragments in this rock are andesite with massive structure, porphyro-afanitic, and allotriomorphic intercrystal relationship, with the composition of the constituents being clay minerals, plagioclase, and mafic minerals. The degree of weathering of this rock is highly weathered.	Dry density values are about 1.5 gr/cm3, and the compressive strength value is 1.4 MPa.
Extremely weathered tuff breccia	Brown in color with a massive structure, fragments consist of andesite with 1 – 8 cm in size. The matrix comprises clay minerals, plagioclase, and mafic minerals <1 mm in size, sub-angular to sub-rounded grain shape, and poor sorting. Fragments in this rock are andesite with massive structure, porphyro-afanitic, and allotriomorphic intercrystal relationship, with the composition of the constituents being clay minerals, plagioclase, and mafic minerals. The degree of weathering of this rock is highly weathered.	Dry density values are about 1.2 gr/cm3, and the compressive strength value is 1 MPa.

<2 mm to about 3 mm, moderate consolidation level, sub-rounded to sub-angular grain shape, with a composition of hornblende, plagioclase, clinopyroxene, lithics, and clay minerals. Lithics in this rock matrix are rocks that have grain sizes up to about 3 mm, have a holocrystalline crystallinity texture, fine crystal size, porphyritic, hypidiomorphic, with a composition of plagioclase, hornblende, and clay minerals. Based on this analysis, the name crystal tuff (Fisher, 1966) was obtained as the matrix of the tuff breccia in this unit. From this information, it can be known that this breccia is a breccia of primary volcanic products. Documentation of the outcrops, hand specimen samples, and microscopic observations of the tuff breccia can be seen in Figure 10. At the surface, the tuff breccia is dominantly extremely weathered. Highly weathered tuff breccia is only observed at the river slopes. Engineering properties of the weathered tuff breccia are shown in Table 3. Based on the International Society for Rock Mechanics and Rock Engineering (ISRM) (1978), the tuff breccia is classified as a very weak rock.

FIGURE 10. (a) Outcrop of tuff breccia. (b) hand specimen sample of the fragment of tuff breccia. (c) and (d) Microphotographs of tuff breccia. Hbl = hornblende, Plg = plagioclase, Cly = Clay, Ox = oxide minerals, and Lth = Lithic.

3.3 Geological structure characteristics

The toll road and tunnel location are more than 10 km from the Merapi-Merbabu and Rawapening Fault, identified by The National Center for Earthquake Studies (2017) (Figure 3). In addition to these two massive active faults, the geological structures found in the study area are compressional joints. Based on the analysis using rose diagrams, the main orientations of the compressional joints are northwest-southeast and northeast-southwest (Figure 11), consistent with the morphological alignment pattern in the study area and its surroundings based on DEM image analysis (Figure 6b).

4 POTENTIAL GEOLOGICAL HAZARD

Although the study area consists dominantly of hilly morphology and extremely weathered rocks, landslides are rarely observed (Figure 4). Landslides in the study area are usually shallow on river slopes less than 5 meters high. One of the largest landslides found was close to the outlet of tunnel B (Figure 5). This may be attributed to the land use and relatively high friction angle of the weathered pyroclastic rocks comprising this area. The study area has been developed mainly as a plantation area. Cut slopes are typically made less than 2 m high, and high slopes of more than 5 m are rarely observed. Previous authors indicate that the weathering of pyroclastic rocks produces soils with relatively high friction angles, implying that high slopes can be stable under natural conditions. For instance, Wesley (1979) reported that the friction angle values of soils from pyroclastic rocks in Indonesia range from 31 to 38°. Keam (2008) reported that the friction angle values of soils from pyroclastic stones in New Zealand range from 50 to 56°. Moon *et al.* (2015) reported that friction angle values of soils from pyroclastic rocks in New Zealand range from 29 to 41°. However, Moon (2016) states that the soils produced from weathering pyroclastic rocks can be susceptible to remolding. Therefore, cut slopes for road and tunnel constructions must be designed to prevent change in the soil state (from natural to remoulding state) by considering landslide-triggering factors, such as rainfall and earthquakes.

5 CONCLUSION

The study area, where the toll road and tunnel will be constructed, consists of two geomorphologic units of steep-slope volcanic hills and

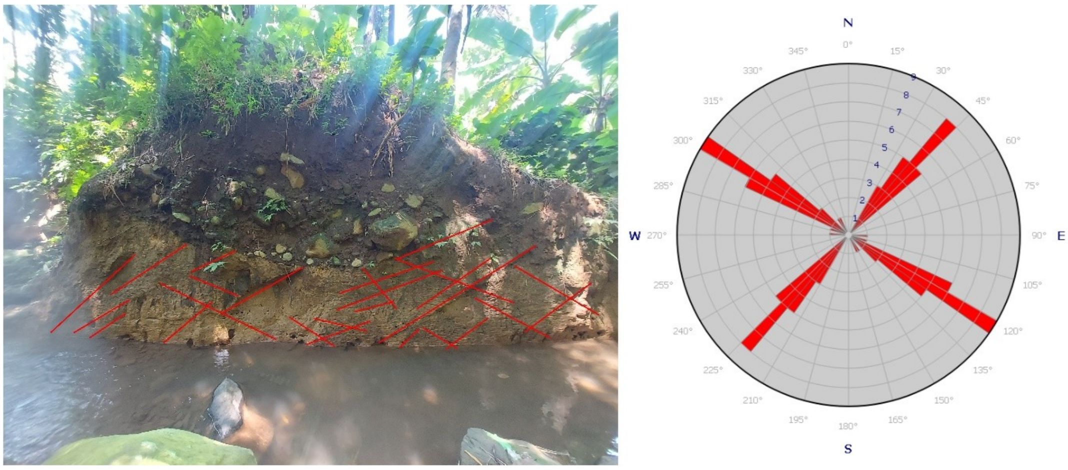

FIGURE 11. Typical compressional joints in the study area and the rose diagram showing the primary orientation of the joints.

gentle-slope volcanic hills and is located near an ancient volcanic crater. The study area has a parallel flow pattern with an orientation consistent with the NW–SE and NE–SW morphological alignment pattern. The study area's morphological alignment is mainly controlled by erosion rather than tectonics.

The study area dominantly consists of extremely weathered tuff with low compressive strength. The toll road and tunnel location are more than 10 km from the Merapi-Merbabu and Rawapening Fault. Other geological structures in the study area are extensional joints, which have an orientation consistent with morphological alignment. Although the study area consists dominantly of hilly morphology and extremely weathered rocks, landslides are rarely observed. This may be attributed to the land use and relatively high friction angle of the weathered pyroclastic rocks comprising this area. The soils from weathering pyroclastic rocks in the study area may be susceptible to remoulding. Therefore, cut slopes made for road and tunnel constructions must be designed to prevent changes in the soil state by considering landslide-triggering factors, such as rainfall and earthquakes.

Acknowledgements The authors would like to thank the management of PT Jasamarga Jogja Bawen (PT JJB) for permission to conduct research and publish some of the data on the borehole investigation. Thanks also to Dr. Esti Handini of the Geological Engineering Department of UGM for reviewing the petrographic analysis. The authors also thank Nur Itsnaini and Mochammad Farhan Dzaki for their support in field data collection and discussions.

REFERENCES

American Society for Testing and Material. (2016). Standard Test Method for Determination of the Point Load Strength Index of Rock and Application to Rock Strength Classifications (ASTM D5731-16). URL: https://www.astm.org/d5731-16.html.

Bogie, I., and Mackenzie, K.M. (1998). The Application of a Volcanic Facies Model to an Andesitic Stratovolcano Hosted Geothermal System at Wayang Windu, Java, Indonesia. Proceedings 20th NZ Geothermal Workshop, New Zealand, 265–270.

Dearman, W.R. (1991). Engineering Geological Mapping. Butterworth-Heinemann.

Fisher, R. V. (1966). Rocks are composed of volcanic fragments and their classification. Earth-Science Reviews, 1(4), 287–298. DOI: 10.1016/0012-8252(66)90010-9.

Gonzalez de Vallejo, L., and Ferrer, M. (2011). Geological Engineering. CRC Press.

International Society for Rock Mechanics and Rock Engineering. (1978). Suggested methods for quantitatively describing discontinuities in rock masses. International Journal of Rock Mechanics and Mining Science & Geomechanics Abstracts, 15, 319–368. DOI: 10.1016/0148-9062(78)91472-9.

Keam, M.J. (2008). Engineering geology and mass movement on the Omokoroa Peninsula, Bay of Plenty, New Zealand. [Unpublished Master Thesis]. University of Auckland.

Moon, V.G., Lowe, D.J., Cunningham, M.J., Wyatt, J.B., Churchman, G.J., de Lange, W.P., Mörz, T., Kreiter, S., Kluger, M.O. & Jorat, M.E. (2015). Sensitive pyroclastic-derived halloysitic soils in northern New Zealand: Interplay of microstructure, minerals, and geomechanics. In T.Rotonda, M. Cecconi, F. Silvestri & P. Tommasi (eds), Keynote Lectures: Volcanic Rocks and Soils (pp. 3–21). Taylor and Francis Group. DOI: 10.1201/b18897-3.

Moon, V. G. (2016). Halloysite behaving badly: geomechanics and slope behavior of halloysite-rich soils. Clay minerals, 51(3), 517–528. DOI: 10.1180/claymin.2016.051.3.09.

Norwegian Tunnelling Society. (2014). Norwegian Tunnelling Technology (Publication No. 23). Norsk Forening for Fjellsprengningsteknikk.

Poedjoprajitno, S. (2011). Photo Geomorphological Map of Java and Madura Islands, Scale 1:1.000.000. Center for Geological Survey.

PT. Cipta Strada-KSO. (2022). Detailed Engineering Design Yogyakarta-Bawen Tunnel (Report No. 066/TUNNEL/JJB/DED/2022/REV0).

The National Center for Earthquake Studies. 2017. Maps of Earthquake Sources and Hazards 2017. The Ministry of Public Works and Housing.

Thandean, R.E., Sumadirdja, H., Richards, P.W., Sutisna, K., & Amin, T.C. (1996). Geological Map of The Magelang and Semarang Sheets, Jawa, Scale 1:100.000. Center for Geological Survey.

van Zuidam, R.A. (1983). Guide to Geomorphologic Aerial Photographic Interpretation and Mapping. ITC Enschede.

Wesley, L. (1977) Shear strength properties of halloysite and allophane clays in Java, Indonesia. Géotechnique, 27, 125–136. 10.1680/geot.1977.27.2.125.